Space-Weather-Driven Geomagnetic- and Telluric-Field Variability in Northwestern Russia in Correlation with Geoelectrical Structure and Currents Induced in Electric-Power Grids

E. Yu. Sokolova[a], *, O. V. Kozyreva[a], V. A. Pilipenko[a, b], Ya. A. Sakharov[c], and D. V. Epishkin[d]

[a]*Schmidt Institute of Physics of the Earth, Russian Academy of Sciences, Moscow, 123242 Russia*
[b]*Geophysical Center, Russian Academy of Sciences, Moscow, 119296 Russia*
[c]*Polar Geophysical Institute, Murmansk, 183010 Russia*
[d]*Northwest (NordWest) Company, Moscow, 108811 Russia*
*e-mail: sokolova@mail.ru

Abstract—The study results of the temporal and spatial variability of geomagnetic and telluric fields driven by anomalous space weather are presented for the central and eastern parts of the Fennoscandian shield. Data from the Scandinavian network of geomagnetic observations IMAGE are analyzed together with the measurements of the geomagnetically induced currents (GIC) in nearby electric power lines of Karelia and the Kola Peninsula, as well as synthesized telluric fields. To synthesize telluric fields from the observed geomagnetic variations, we use magnetotelluric impedance estimates obtained during the BEAR electromagnetic sounding experiment in Fennoscandia. A comparison of the spectral composition of geomagnetic, telluric, and GIC variations in various sites and for various space weather events has shown that time derivative of the geomagnetic field (dB/dt), which is commonly used as a measure of GIC disturbances, does not fully control the latter. The analyzed telluric fields and observed GICs demonstrate a significant dependence on the induction response of the electrically conducting Earth interiors, the character of which varies greatly in different geological domains of the Fennoscandian shield. The regional spatial variations in the telluric field and GICs caused by the geoelectric structure heterogeneity are superimposed on the regular decreasing trend in their amplitudes with increasing distance from auroral latitudes. Based on magnetotelluric sounding data, estimates of the extreme values of telluric fields during geomagnetic storms and substorms are obtained for different sites, which is the key information for predicting GICs in regional power lines.

Keywords: space weather, geomagnetic storms and substorms, telluric fields, geomagnetically induced currents (GICs), magnetotelluric impedance, geoelectric inhomogeneities of the Earth's crust, Fennoscandian shield

DOI: 10.1134/S000143381911015X

INTRODUCTION

The dynamics of solar–terrestrial interactions define the "space weather" concept as a state of the near-Earth plasma and, at the same time, as a set of factors influencing all spheres of life on Earth, from technological to biological (Kleimenova and Kozyreva, 2008). Along with solar radiation, the most effective factors include geomagnetic activity, i.e., variations in the Earth's magnetic field on different time scales; these variations strongly depend on the parameters of the solar wind and interplanetary magnetic field (Yermolaev et al., 2005). Geomagnetic activity reaches its peak during magnetic storms, which are the responses of the geomagnetic field to powerful solar flares (solar coronal mass ejections) or high-speed solar wind streams. Magnetic storms can be characterized by a sudden onset, long duration (up to several days), and broadband high-amplitude field variations (up to hundreds and thousands nanoteslas). In addition to the negative impact on radio communications and GPS navigation, these extreme manifestations of space weather are very dangerous for the functioning of space and ground-based technological systems and infrastructure objects, since abrupt time variations in the geomagnetic field (dB/dt) generate strong geomagnetically induced currents (GICs) in technological conductors (Lanzerotti, 2001; Knipp, 2015; and others).

Intensive GICs can cause malfunctions of railway equipment (Sakharov et al., 2009; Eroshenko et al., 2010), as well as damage and actively corrode pipelines (Pulkkinen et al., 2001; Cannon et al., 2013). In addition, there are numerous examples of serious consequences of space weather disturbances for extended high-voltage power grids, and this, apparently, is the strongest hazard to industrial technological systems. For example, one can mention the unprecedented

regional power outage (blackout) in Canada in 1989 that lasted for hours due to malfunctions in high-voltage power lines connecting Quebec with remote hydroelectric power stations due to GICs (Allen et al., 1989); severe power outages in Sweden during a powerful magnetic storm on October 31, 2003 (Pulkkinen et al., 2015); and a number of other similar events. Geomagnetic variations induce electric fields (geoelectric, or telluric fields) in the conducting Earth, which generate EMF in grounded low-impedance conductors and, therefore, create additional low-frequency currents in power lines. Quasi-constant GICs are especially dangerous for high-voltage transformers: they cause semiperiodic saturation of the cores, an increase in harmonics, and overheating and damage to the windings. The sensitivity of transformers to GICs varies; there is no general rule on how strong the current should be in order to cause damage, since a GIC of only a few amperes can be sufficient to disrupt the linear mode of some power transformers (Vahnina et al., 2015).

Integration of high-voltage power lines into unified power systems, increased loads, and transition to low-impedance lines with higher voltages increase the likelihood of failures during space-weather events. In this case, a negative economic effect is caused not only by equipment breakdowns, but also by strong, far-transmitted power surges, which are the most frequent consequences of geomagnetic storms (Pulkkinen et al., 2017). Therefore, even if the equipment of the energy infrastructure is not damaged during extreme space weather events, the impact of GICs on regional power systems and the global economy can still be quite noticeable (Forbes and Cyr, 2004).

Strong GICs can be generated not only by systems of large-scale auroral currents, but also by relatively weak and small-scale, but fast, processes accompanied by abruptly changing electromagnetic fields (Viljanen et al., 2001; Belakhovsky et al., 2018). Considering these phenomena, information on GICs is very important for basic research to identify the fine structure of fast geomagnetic variations during storms and substorms.

It is usually assumed that the GIC intensity is proportional to the time derivative of the geomagnetic field: $J \sim dB/dt$ (Viljanen, 1997). However, strictly speaking, for a closed loop with ohmic resistance, this relationship is valid only in free space. In real situations, the GIC circuit is formed by transmission lines, grounding contacts, transformers, and the conducting Earth; in most cases, the electrical parameters of these elements, as well as their frequency dependence, are not known exactly. Obtaining direct information about EMF-generating geoelectric fields requires considerable effort. While variations in the geomagnetic field are monitored by means of a global magnetometer network (more than 300 continuously recording stations), regular observations of telluric fields,

and especially GICs, are quite rare. In addition, information on GICs, as a rule, is the property of commercial companies and is not available to the world scientific community for in-depth analysis.

Comprehensive geophysical studies of GIC-related problems are gaining more and more scope. This is confirmed by the recent sharp increase in the number of publications on GICs in major geophysical journals (Cannon et al., 2013; Torta et al., 2014, 2017; Pulkkinen et al., 2015; Kelbert et al., 2017; Belakhovsky et al., 2018; Kozyreva et al., 2018; and others) and attention to this problem from the industry (Love et al., 2016). At the same time, despite the fact that the most intense GICs (more than a hundred amperes) were measured during magnetic storms and substorms in auroral regions, studies of such space-weather effects are also carried out in midlatitude regions as a response to the need for comprehensive protection of important infrastructure objects taking into account possible extraordinary effects of fast magnetospheric events (Torta et al., 2014, 2017; Kelly et al., 2017).

The most actively developing areas of GIC studies today include the creation of basic regional forecast maps of extreme values of induced geoelectric fields; these maps are the key data for estimating and predicting GICs. The first such maps were compiled for the United States based on statistical estimates of extreme amplitudes of geomagnetic variations with the use of an array of magnetotelluric (MT) impedances of the EarthScope national geophysical sounding project covering most of the country (Love et al., 2016). In addition, approaches to the calculation of actual telluric responses are actively being improved taking into account the three-dimensionality of geoelectric structures and adequate models of an inhomogeneous external source of their anomalous excitation (Puthe and Kuvshinov, 2013; Alekseev et al., 2015; Kelbert et al., 2017; Ivannikova et al., 2018; Dimmock et al., 2019; and others). Just as relevant are the introduction of experimental GIC measurements into research practice, their analysis, and attempts to estimate GICs by telluric fields taking into account the topology and specific parameters of a power grid (Torta et al., 2014, 2017).

The aim of our studies is to develop an understanding of the actual relationships between variations in the geomagnetic field B (including its derivative dB/dt), telluric field E, and geomagnetically induced current J based on the study of variations in geomagnetic and telluric fields due to space weather events in the Central and East Fennoscandia. The focus of this paper is experimental material that characterizes the high-latitude regions of northeastern Russia, which are distinguished by a developed industry and infrastructure, strong contrasts of the crustal conductivity and, most importantly, an established system of GIC measurements in the extended power lines of Karelia and the Kola Peninsula (Sakharov et al., 2007). Considering the latter, we were able to supplement the analysis of
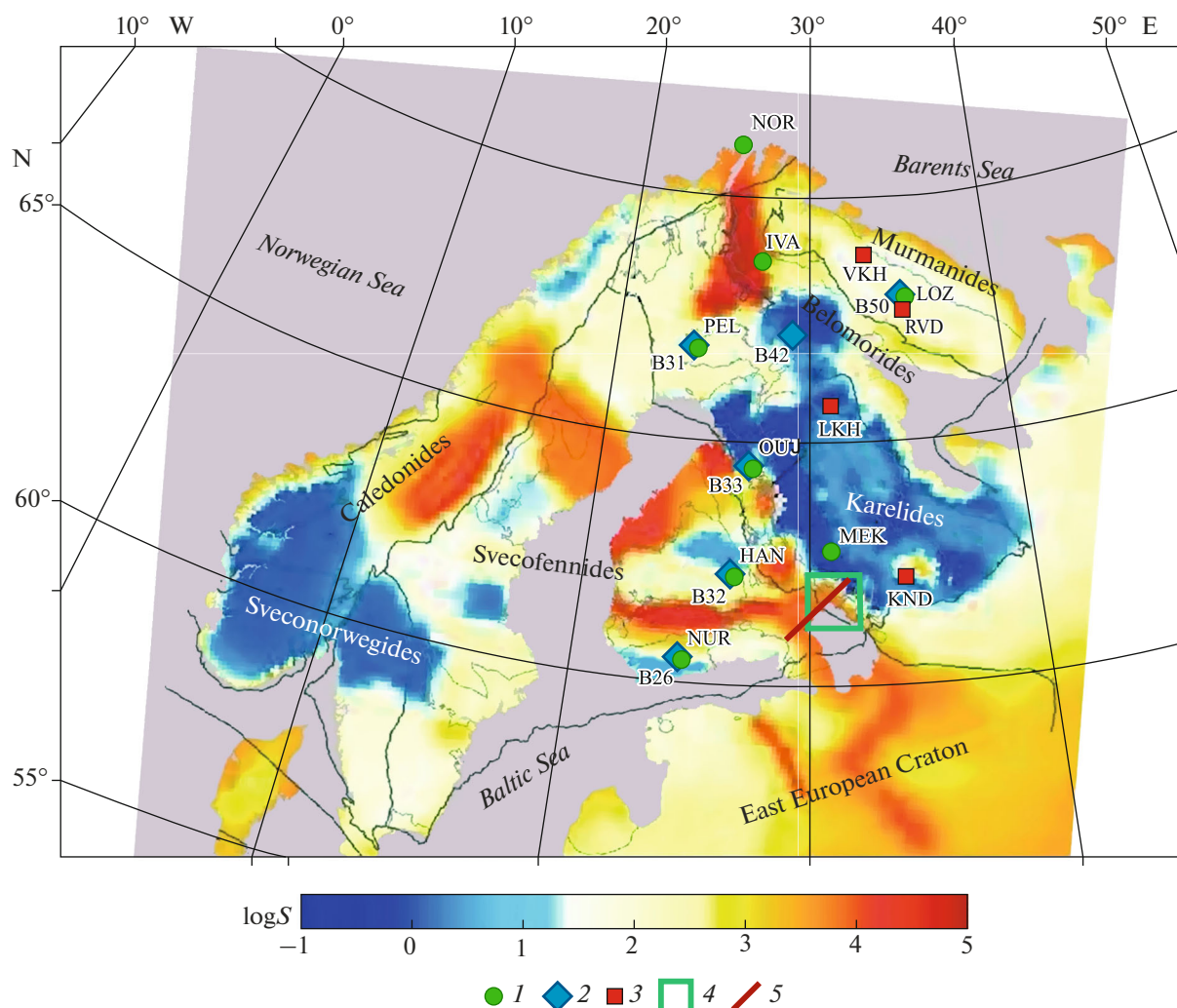
Fig. 1. Locations of (*1*) the geomagnetic observation sites of the IMAGE network, (*2*) the MT deep sounding sites of the BEAR project, and (*3*) the stations for recording GICs in the power transmission lines on the map of the integrated longitudinal conductivity *S* (measured in siemenses) of the Earth's crust of the Fennoscandian shield with the designation of the main tectonic domains (according to (Korja et al., 2002) with modifications). (*4*) The region of Fig. 14; (*5*) Vyborg–Suoyarvi profile of MT soundings.

electromagnetic fields with the GIC measurements at the stations closest to the geomagnetic observation sites of the Scandinavian IMAGE network, which provides the basic material for the study (Fig. 1). The absence of observations of telluric fields during the events under study was compensated for by the possibility of synthesizing them using a specially developed software from the observed geomagnetic variations in the time domain and known magnetotelluric responses—impedance tensors from the data array of areal deep sounding of the territory of the Fennoscandian shield (international BEAR project (Korja et al., 2002)). The objectives of the study were to analyze the spatial changes in the anomalous geomagnetic and telluric responses due to the significant difference of the deep electrical conductivity structure of various geological domains in the east of the Fennoscandian shield (see Fig. 1). In addition to the BEAR data, we used materials of recent detailed MT soundings in the Northern Ladoga region (Sokolova et al., 2016) on a profile intersecting the junction zone of the Archean Karelian craton and the Paleoproterozoic Svecofennian collision orogen, which have contrasting geoelectric properties (see Fig. 1).

GEOMAGNETIC, MAGNETOTELLURIC, AND GIC DATA AND METHODS OF THEIR ANALYSIS

The system for monitoring GICs in power transmission lines was deployed on the Kola Peninsula and in Karelia by the Polar Geophysical Institute, Russian Academy of Sciences, and the Center for Physical and Technical Problems of Energy of the North, Kola Science Center, Russian Academy of Sciences (Sakharov
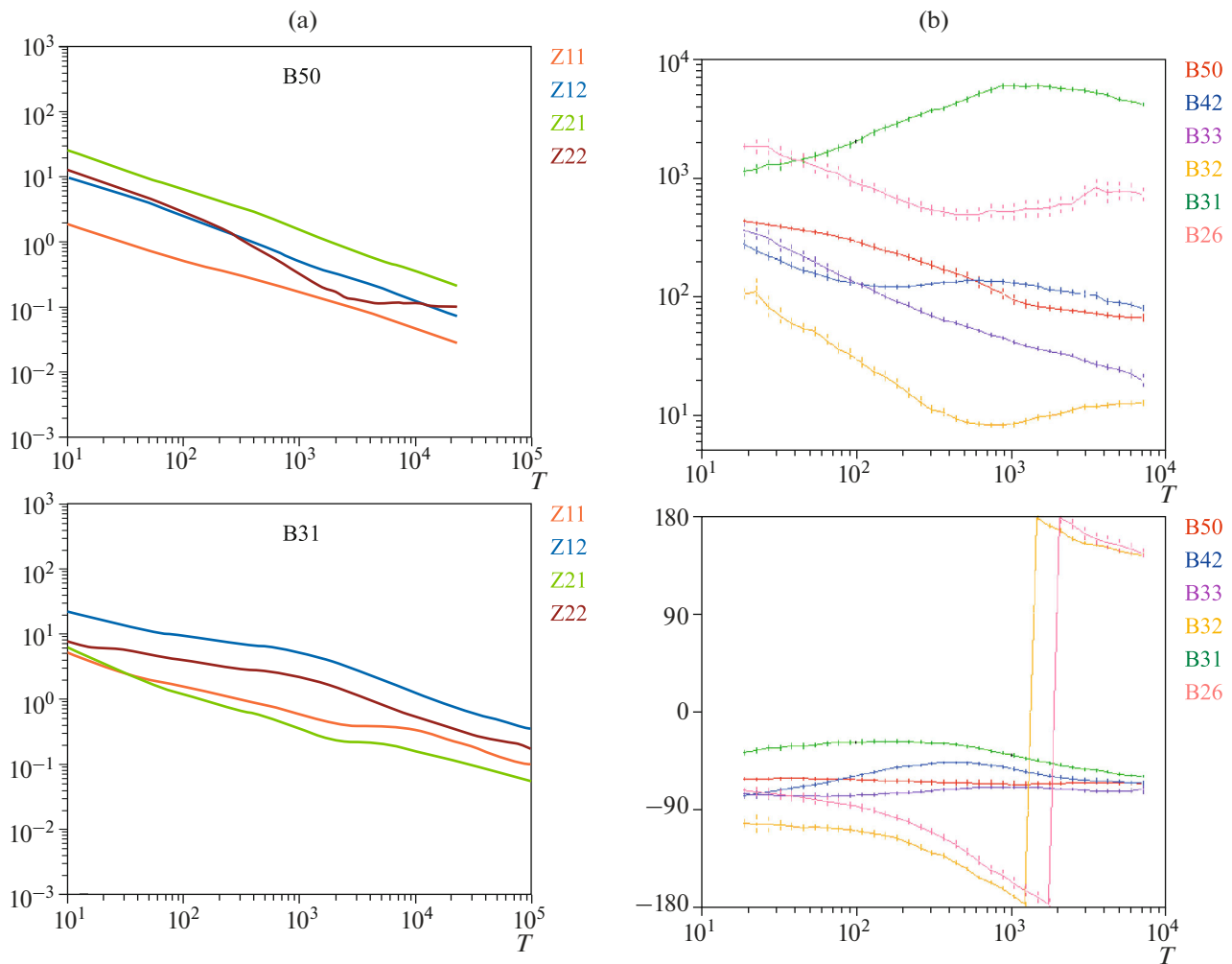
Fig. 2. The dependences of the magnetotelluric transfer functions on the period T (s). (a) Amplitudes of the elements of the impedance tensors $Z_{i,j}$ (in practical units mV/(km nT) at the BEAR project stations B50 and B31), where i is north and j is east; (b) northern components of apparent resistivity $\rho_{i,j}$ (Ohm m) $= 0.2T |Z_{ij}|^2$ and impedance phase $\mathrm{arg}Z_{i,j}$ at the BEAR project stations; (c) amplitudes of the elements of the impedance tensors $Z_{i,j}$ (top panel) and $Z_{j,i}$ (bottom panel) at five points of the Vyborg–Suoyarvi profile. Location of the stations see in Fig. 1 for Figs. 2a and 2b and in Fig. 14 for Fig. 2c. Hereinafter, geomagnetic coordinates are used unless otherwise specified.

et al., 2007). It includes four GIC recording stations on the main power transmission line (330 kV) (see Fig. 1). Each station records a quasi-constant current in the dead-grounded neutral of the autotransformers with a sampling rate of 1 min using specially designed economical recorders that allow measurements without breaking the integrity of the circuits at the substation.

Local geomagnetic variations were monitored using 10-s data at the stations of the Scandinavian geomagnetic observation network IMAGE (http://space.fmi.fi/image/www/) located closest to the GIC recording stations (see Fig. 1). To characterize the general level of geomagnetic disturbances in the studied region, we used the regional index EI (available at the website of the Finnish Meteorological Institute), which mainly characterizes the activity of the auroral electrojet, which is the most typical phenomenon related to space weather in the region (Pellinen and Heikkila, 1984).

Telluric fields were synthesized from selected geomagnetic variation records using magnetotelluric impedance estimates obtained at the BEAR sounding stations in the period range from 8 s to 8000–55000 s (Varentsov et al., 2003) (Figs. 2a, 2b). The detailed analysis of telluric responses at the boundary of the geological and structural domains of Eastern Fennoscandia also involved the broadband impedance dependences at the stations of the Vyborg–Suoyarvi profile in the Northern Ladoga region (Sokolova et al., 2016) (Fig. 2c).

The algorithm for synthesis of the telluric field $E(t)$ from the geomagnetic field $\Delta B(t) = \{X(t), Y(t)\}$, where X is its northern geomagnetic component and Y is eastern geomagnetic component, was based on the funda-

mental magnetotelluric dependence of electric $E(f)$ and magnetic $B(f)$ fields in the frequency domain via the total complex tensor of impedance $Z(f)$ (Berdichevsky and Dmitriev, 2009):

$$\begin{pmatrix} E_i(f) \\ E_j(f) \end{pmatrix} = \mu_0^{-1} \begin{pmatrix} Z_{ii} & Z_{ij} \\ Z_{ji} & Z_{jj} \end{pmatrix} \begin{pmatrix} X(f) \\ Y(f) \end{pmatrix}, \qquad (1)$$

where μ_0 is the magnetic permeability of the vacuum.

The Fourier transform was applied to overlapping consecutive segments (sliding time windows) of the analyzed geomagnetic field record to obtain a set of spectral estimates $\Delta B(f)$ and, using formulas (1), the corresponding estimates of the telluric field $E(f)$. The inverse Fourier transform was performed for each time window. Thus, for the time instant corresponding to the middle of each window, there were several estimates of the electric field, which were averaged to stabilize the calculation of the final time series of the synthetic electric field $E(t)$ corresponding to the magnetic record. The software implementation of the algorithm was based on the practice of modern developments of new methods for estimating the MT transfer functions (Epishkin, 2016) and successfully demonstrated its correctness and efficiency on the synthetic magnetic and electric time series of the COMDAT project (Ernst et al., 2001).

Further, for a number of distinct space weather events, selected basing on the availability of GIC records, the synthesized telluric fields were analyzed together with geomagnetic and GIC data. The analysis was carried out using spectral and correlation methods. The GIC materials and data of the IMAGE and BEAR projects were grouped depending on their availability at the observation points located most closely to each other (see Fig. 1). For example, we simultaneously analyzed the synchronous records from LOZ and RVD stations, which were supplemented with synthetic telluric fields calculated from the MT impedance at B50 station of the BEAR project array, and the materials of IVA and VKH stations located at close geomagnetic latitudes (relying on the least distant MT stations B42 or B50 for the synthesis of the telluric component). The variations at the MEK station of the IMAGE network approximated geomagnetic fields at the sounding points of the northern segment of the MT profile in the Northern Ladoga.

RESULTS

Magnetic Storm of November 12–14, 2012

A series of short-term amplifications of auroral currents occurred on November 14, 2012, in the interval of 00−04 UT during a strong magnetic storm ($|SYM-H| > 100$ nT); this was marked by the local electrojet intensity index EI reaching ~150 nT (Fig. 3a). Two pulses with the largest amplitudes associated with substorm activations occurred at IVA and LOZ stations around 01 UT and 02:20 UT. At a lower latitude
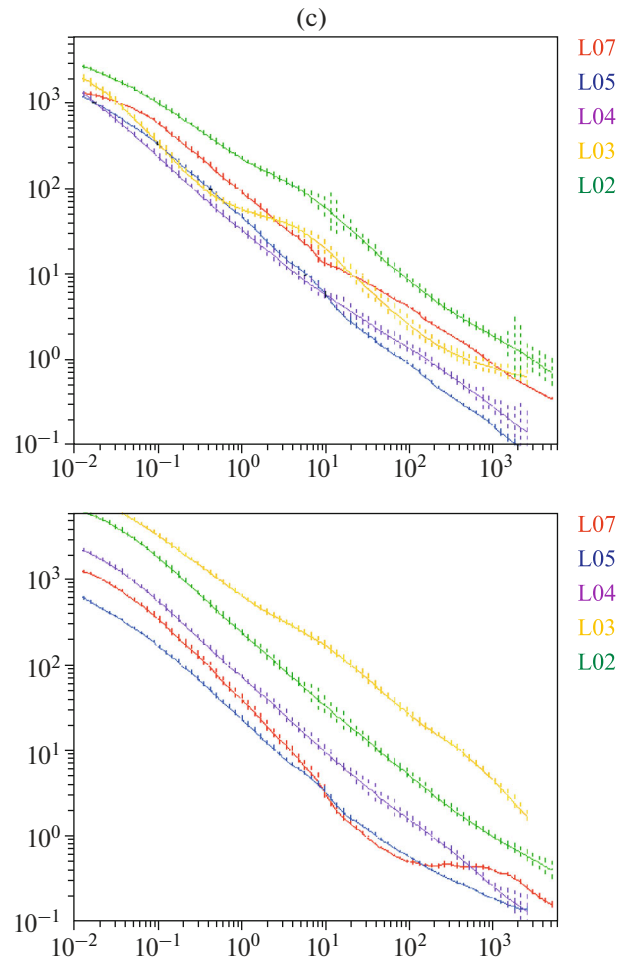

Fig. 2. (Contd.)

(OUJ), the maximum magnetic disturbance was observed at approximately 01:50 UT. The peak of the EI index at ~03:30 UT is associated with activation that was remote from the stations considered.

In Fig. 4, the GIC intensity J at VKH is compared with the variations in the magnetic field component X, time derivative dX/dt, and telluric fields E_x and E_y at IVA station (the telluric fields are synthesized using the impedance at B50 station). The J peaks are coherent with the surges of dX/dt (up to ~100 nT/s) and E-field (up to several V/km).

Even a visual assessment of Fig. 4 reveals that the fluctuations of $dX/dt \equiv X'$ are more high-frequency when compared with the variations in E and J. This conclusion is confirmed by the spectral analysis results illustrated in Fig. 5 by the spectra of geomagnetic and telluric fields, as well as GIC, normalized for a more detailed comparison.

The spectral components at frequencies of ~4 mHz and ~6 mHz have increased amplitudes for $J(f)$ and $X'(f)$. They are caused by the contribution of fast fluctuations in the Pi3 range that participate in the amplifica-

(a)
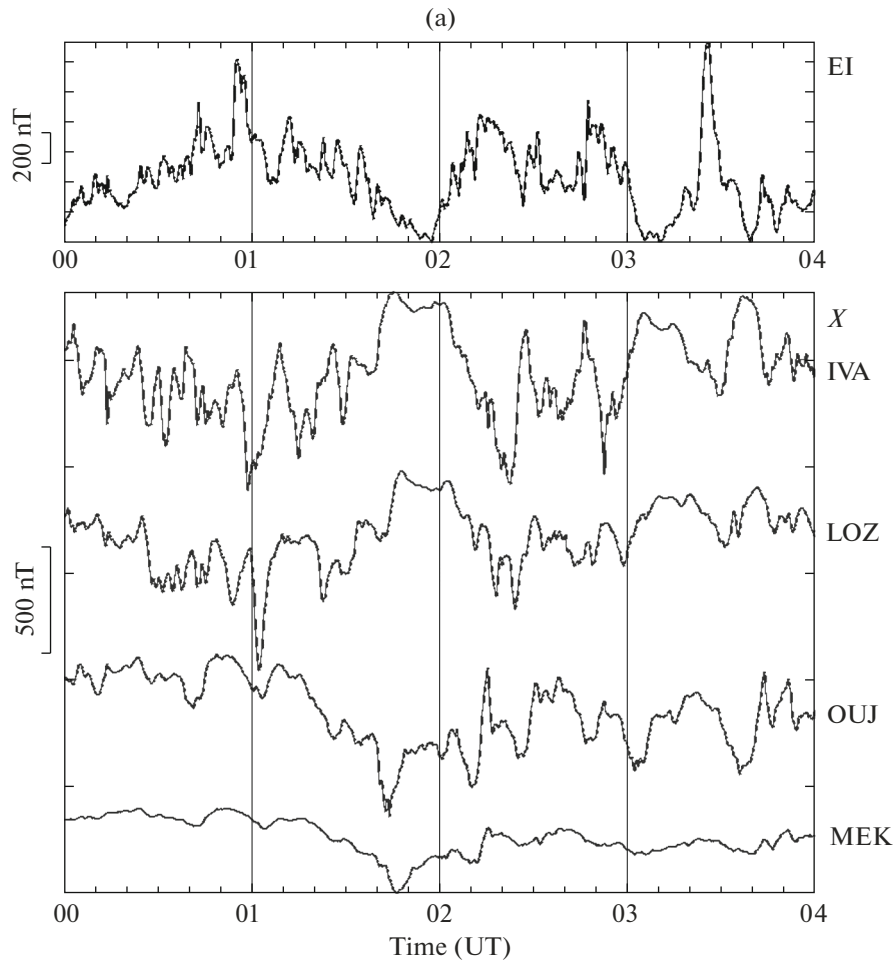
Fig. 3. Variations in the geomagnetic field and GIC intensity at night (00−04 UT) during the magnetic storm of November 14, 2012. (a) Variation in the regional index of geomagnetic activity EI(*t*) and *X*(*t*) component (geomagnetic north) of the magnetic disturbance at stations IVA, LOZ, OUL, and MEK of the Scandinavian IMAGE network; (b) variation in the GIC intensity *J*(*t*) at stations VKH, RVD, LKH, and KND. See the positions of the stations in Fig. 1.

tion of the auroral electrojet. However, overall, the $X'(f)$ spectrum strongly deviates from the $J(f)$ spectrum at higher frequencies (>5 mHz). The latter is closer in character to the $E_x(f)$ spectrum than to the $X'(f)$ spectrum.

Pi3 Pulsations during the Magnetic Storm of June 29, 2013

The magnetic storm of June 27−29, 2013, began around 15 UT on June 27, when the interplanetary shockwave reached the Earth's magnetosphere. Starting from 08 UT on June 28, the interplanetary magnetic field (IMF) gradually changed its direction to the south ($B_z < 0$) and remained stable at approximately −10 nT until 12 UT of June 29. Such an orientation of the IMF, together with the anomalous parameters of the solar wind, led to the development of a strong magnetic storm with the |Dst| index reaching ~120 nT.

The EI index showed a gradual irregular increase during the main phase of the magnetic storm (Fig. 6).

In the period of maximum magnetic activity (00−04 UT), intense irregular variations in EI with a peak-to-peak amplitude of approximately 600 nT are superimposed on the magnetic bay (see Fig. 6). The time scale of these quasiperiodic oscillations, which can be classified as Pi3 pulsations, varies from ~20 min at low latitudes to ~10 min at high latitudes. The most intense variations are observed at OUJ.

During this storm, from 01 to 03 UT on June 29, extremely high GIC values were recorded at VKH station (with a peak-to-peak amplitude of oscillations of ~200 A); GICs at other stations were weaker. Each Pi3 pulse was accompanied by localized GIC pulses and variability of the magnetic and telluric fields (Fig. 7).

For a detailed comparison of the spectral characteristics of GICs and natural electromagnetic fields, we use the observation data from two stations, RVD and LOZ, located in the immediate vicinity of each
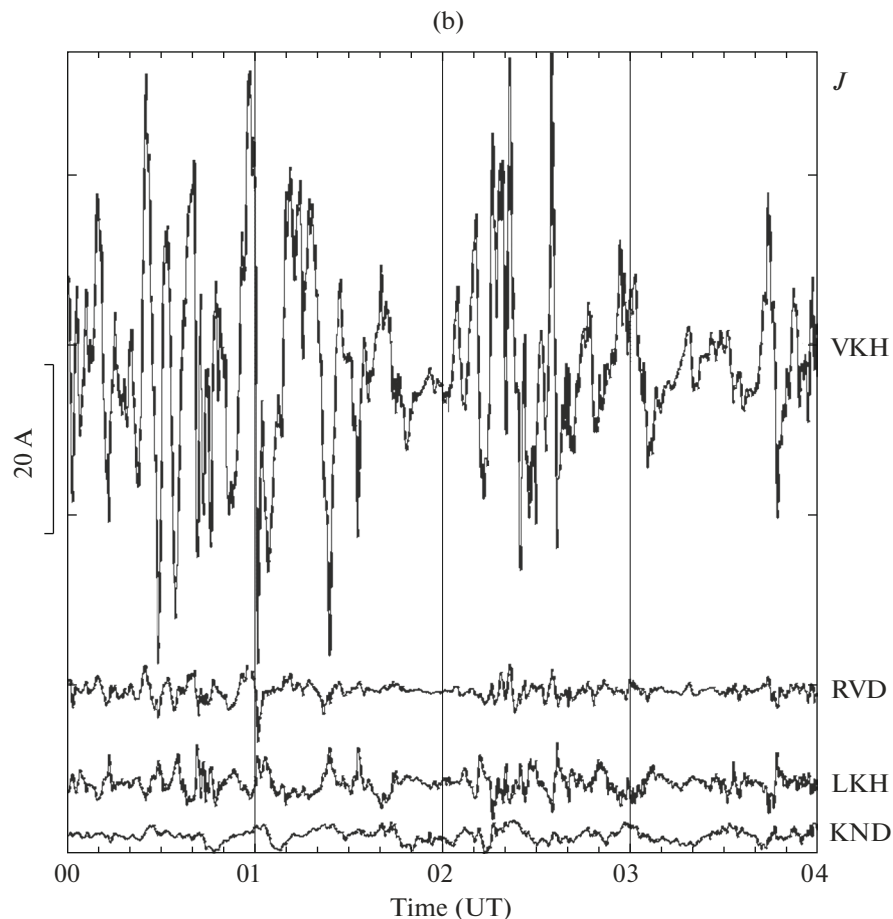
(b)

Fig. 3. (Contd.)

other, as well as the MT impedance of B50 station, which corresponds to LOZ (see Fig. 1). A visual comparison of J at RVD with X and dX/dt at LOZ and E field at LOZ/B50 (Fig. 8) shows that the variations in X for the analyzed interval correlate with the variations in GICs no worse than the time derivative dX/dt itself. This fact is confirmed by the data of spectral analysis (Fig. 9). The combination of the normalized spectra of all time series demonstrates their general decaying character with some amplification at approximately 4 and 7 mHz; this is associated with the participation of Pi3 pulses in the process, which complicate the magnetic bay. The $X(f)$ spectrum in the high-frequency region is larger than the $J(f)$ spectrum. At the same time, the $E_x(f)$ spectrum is closer to the $J(f)$ spectrum (for $f > 7$ mHz).

Substorm of October 6, 2015

Regarding the results of the data analysis for this typical substorm (Fig. 10), it appears important for subsequent discussion to demonstrate the following fact, which is similar to that revealed for the storm of June 27–29, 2013: there is a significant increase in the amplitude of the E_x component of the telluric field at PEL when compared with the same data at other stations. In this case, it should be noted that the geomagnetic fields at PEL and IVA are similar in the level of disturbance; the intensity of variations in E_y is also comparable (see Figs. 10, 11).

The data of IVA and VKH stations for this substorm (Fig. 12) confirm the earlier conclusion about the lower frequency character of the GIC and E_x variations in general when compared with the dX/dt variations inducing them.

DISCUSSION OF THE RESULTS

Generalized Model of the GIC Electric Circuit of a Grounded Power Transmission Line

In the majority of GIC-related studies, the current intensity values J were usually only estimated by their proportional dependence on the rate of change of the geomagnetic field: $J \sim dB/dt$ (Viljanen, 1997). The transition from the above formulation, which is valid only in free space, to more realistic versions of this dependence can be made based on the analysis of a
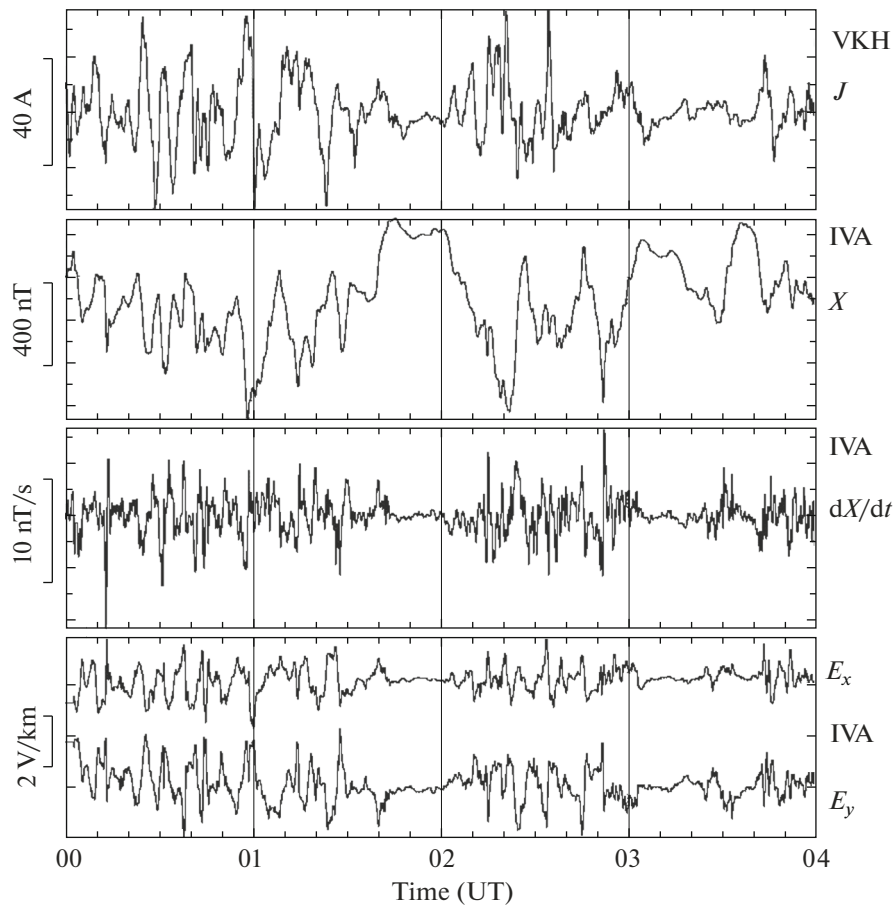
Fig. 4. GIC intensities $J(t)$ at VKH station, variations in the northern component of the magnetic field $X(t)$, time derivative $dX/dt(t)$ at IVA station, and telluric fields $E_x(t)$ and $E_y(t)$ at IVA station (the latter are synthesized using the impedance at B50 station) during the strong magnetic storm of November 14, 2012, in the interval of 00−04 UT.

generalized model of the GIC circuit (Fig. 13). In this case, the key parameter is the penetration depth of the considered electromagnetic field harmonic (with circular frequency ω) into the conductive Earth, i.e., the thickness of the skin layer $\delta(\omega, \sigma)$ for a homogeneous

Fig. 5. Normalized spectra $J(f)$ at VKH station and $X(f)$, $X(f)$, and $E_x(f)$ at IVA/B50 station (electric fields are synthesized using the impedance at B50 station) for 01−03 UT on November 14, 2012.

underlying half-space with specific electrical conductivity σ (S/m), which is estimated as

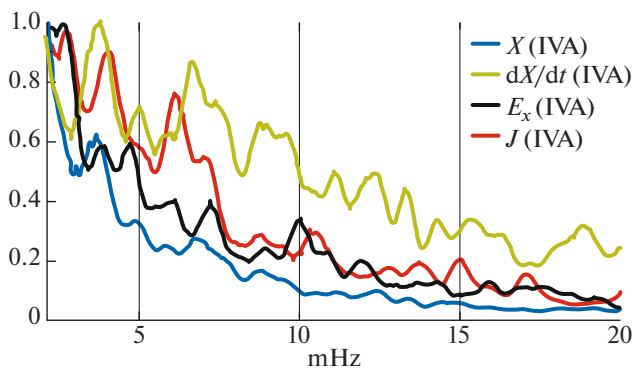$$\delta = \sqrt{2/\mu_0 \omega \sigma}. \tag{2}$$

Based on the Faraday law of electromagnetic induction and Ohm law, the following expression can be obtained for the circuit shown in Fig. 13 regarding the relationship between the current intensity J and the rate of change of the geomagnetic field:

$$2J(L + d + \delta) \sim \frac{\partial B}{\partial t} L(d + \delta). \tag{3}$$

Among the various ratios of the parameters of this dependence, two extreme cases are possible:
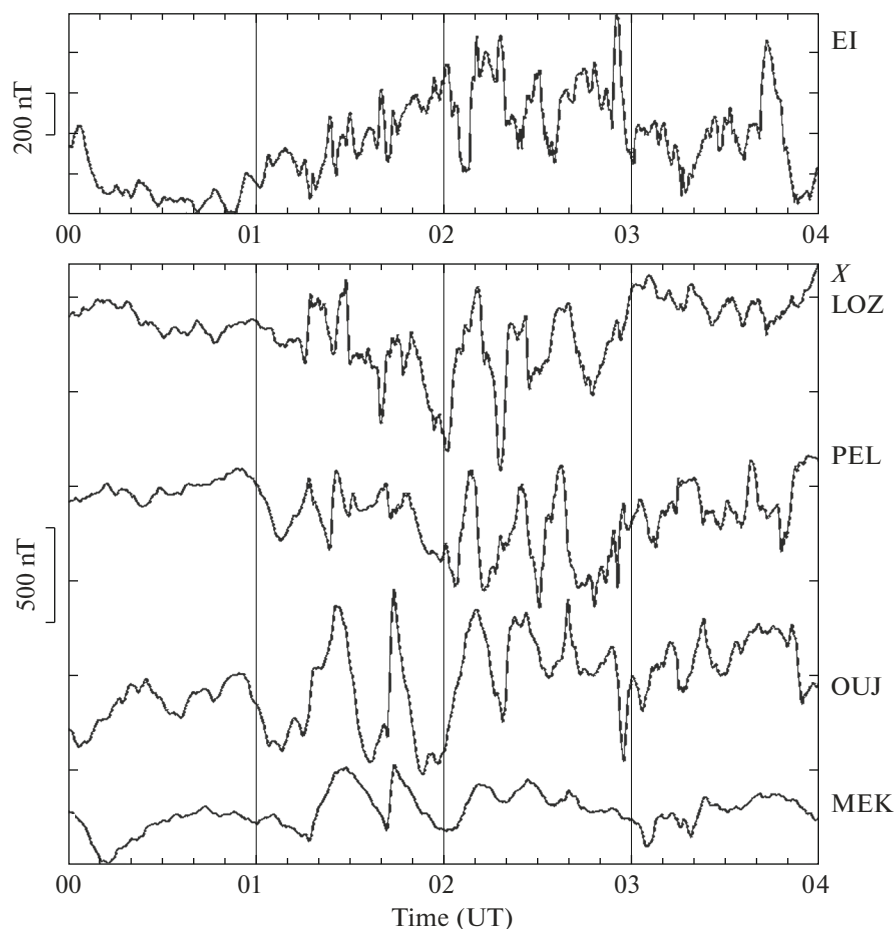
(1) insulating base: a strong skin layer $\delta \gg L$ and $J \sim -i\omega BL$, when the GIC intensity is indeed directly proportional to the time derivative of the geomagnetic field;

(2) conductive base: a thin skin layer $\delta \ll L$ and, taking into account (2), $J \sim -i\omega B\delta(\omega) = -i\sqrt{2/\mu_0\sigma}B\sqrt{\omega}$. In this case, the GIC intensity is proportional to the mag-
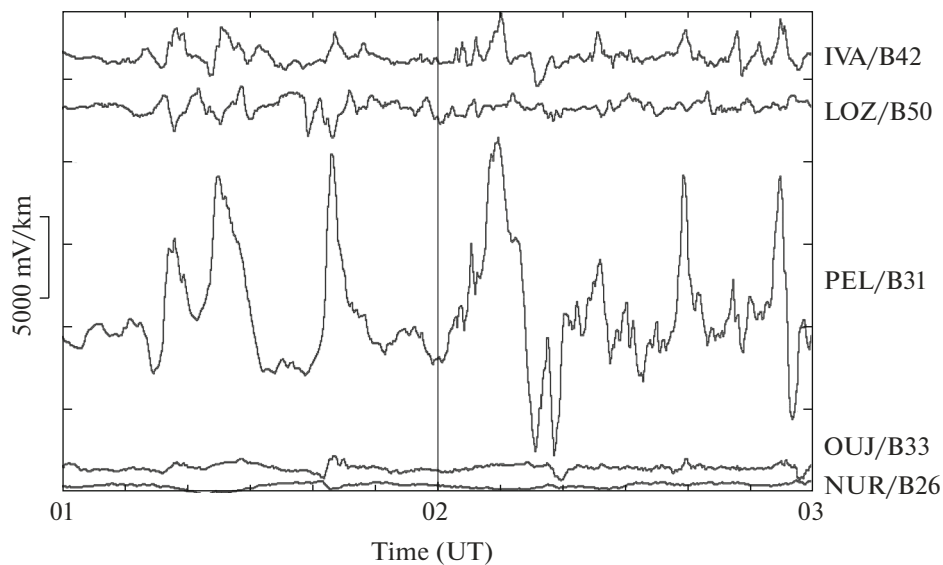
Fig. 6. Variations in geomagnetic activity in the interval of 00−04 UT on June 29, 2013 (EI index, X component of the magnetic field) at IMAGE stations LOZ, PEL, OUJ, and MEK.

Fig. 7. Telluric fields $E_x(t)$ synthesized for the time interval of 01−03 UT on June 29, 2013, from the $X(t)$ components of geomagnetic fields at stations IVA/B42, LOZ/B50, PEL/B31, OUJ/B33, and NUR/B26. The names of the stations after the slash indicate the MT sounding sites of the BEAR project, the impedances of which were involved in the synthesis.
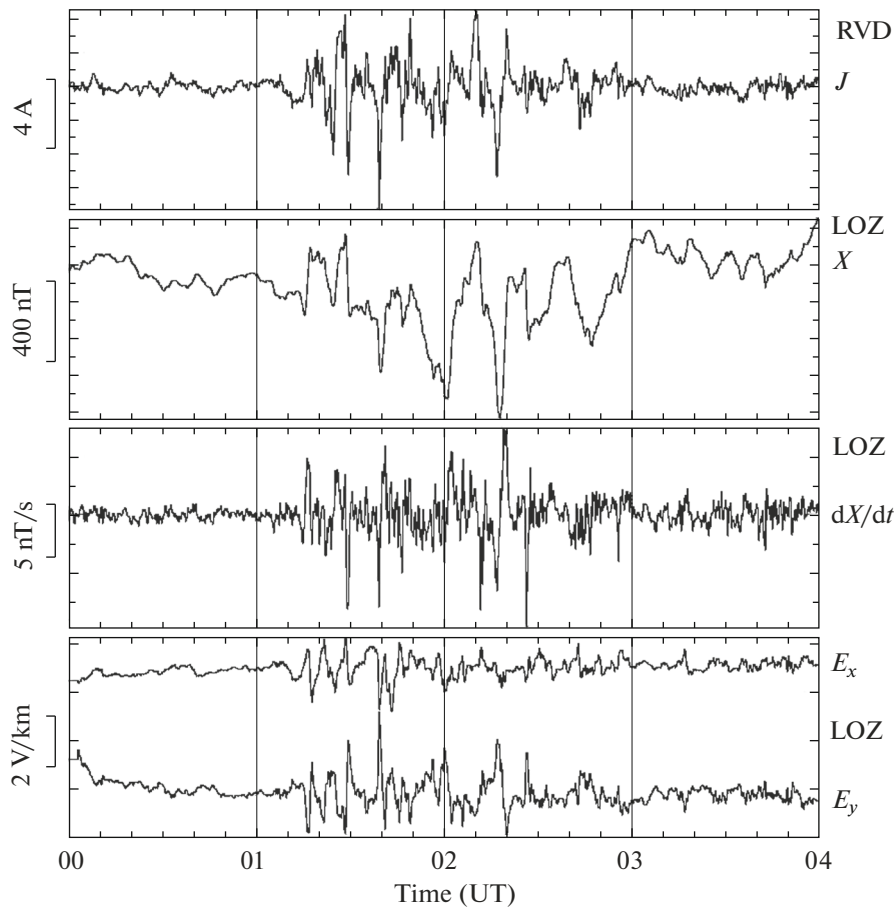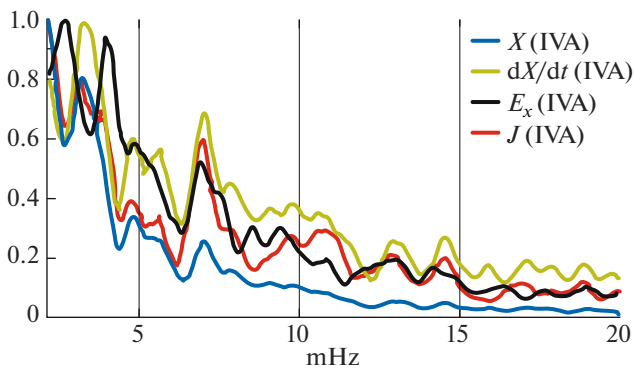
Fig. 8. Comparison of the variations in $J(t)$ at RVD station with the variations in the magnetic component $X(t)$ and its time derivative $dX/dt(t)$ at LOZ station, as well as with the E-fields at LOZ/B50 (synthesis with the impedance at B50 MT sounding station) during the Pi3 event on June 29, 2013. See station locations in Fig. 1.

nitude of the magnetic field and the thickness of the skin layer, but weakly depends on the frequency.

Taking these estimates into account, we can more fully assess the actual relationships between variations in the geomagnetic field B; its derivative dB/dt; the tel-


Fig. 9. Normalized spectra for the period of 01−03 UT on June 29, 2013, for J at RVD station and for X, dX/dt, and E_x at LOZ.

luric field E; and GIC (J), depending on the specific parameters of the key element of the circuit, i.e., the conductive Earth. In case (1), GIC (initially, the telluric field) is mainly determined by the "external" source, dB/dt. In case (2), the role of "internal" sources significantly increases: their induced geoelectric fields can to some extent "dampen" external effects, leveling the amplitudes of high-frequency oscillations in J (or E), depending on δ of the underground medium (in fact, on its MT impedance or electrical conductivity).

Geoelectric Heterogeneities of Fennoscandia as an Important Factor in the Spatial Variability of Telluric Responses and GICs

The geoelectric structure of the Fennoscandian (Baltic) shield has been an object of a great number of studies of different scale; these studies began as early as the middle of the 20th century at the early stages of the development of magnetovariational and magnetotelluric methods of sounding the Earth and continue at present, supplying more and more detailed and reli-
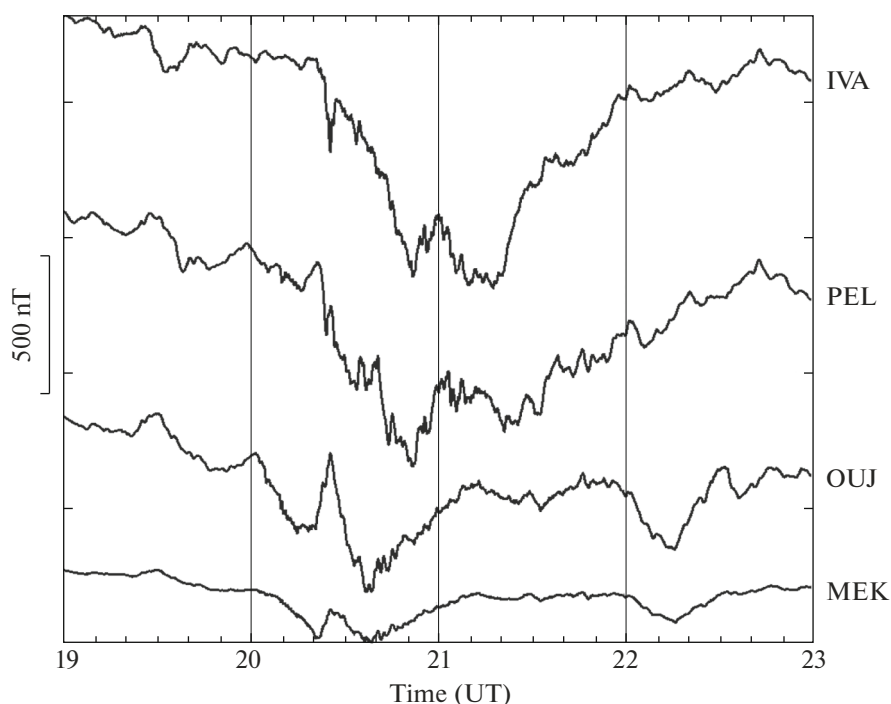
Fig. 10. Variations in the $X(t)$ component of the geomagnetic field for the period of 19−23 UT on October 6, 2015, at IMAGE network stations IVA, PEL, OUJ, and MEK.

able information on the significant heterogeneity of the distribution of electrical conductivity in the Earth's interior (Kovtun, 1989; Korja et al., 2002; Sokolova et al., 2016; Zhamaletdinov et al., 2018; and others). The overviews of the results of geoelectric studies of Kola−Karelia are presented, for example, in (*Glubinnoye...*, 2004; Rokityansky et al., 2018).

Korja et al. (2002) display the geoelectric structure of the Fennoscandian shield as a whole on a scale most suitable for our research. That study discusses the results of the international deep electromagnetic sounding project BEAR and presents the regional model of the electrical conductivity of the Earth's crust. An adapted map (shown in Fig. 1) of the integrated conductivity of a 60-km lithospheric layer shows high contrasts of S across Fennoscandia. Karelides of the Karelian craton, which is composed of Archean granite-greenstone complexes with a resistivity of more than 10^4-10^5 Ohm m, are the most insulating megablock. The Kola megablock, which is also mainly Archean, but subjected to strong tectonic and thermal alteration during the Paleoproterozoic and Paleozoic, has a slightly higher integrated conductivity (average resistivity of the order of 6×10^3 Ohm m). Svecofennides (center and southwest of the shield) have similar geoelectric parameters; however, they contain the largest number of strong regional conductors: volcanogenic and sedimentary mobile belts, which often include metamorphosed graphite−sulfide-containing rock complexes with the highest electronic conductivity σ up to 10^6 S/m.

Turning to the results obtained in our study of geomagnetic, telluric, and GIC variations in the region of Central and East Fennoscandia, we can find convincing examples of the dependence of their amplitude-spectral composition on geoelectrical characteristics at the measuring stations (skin layer δ, MT impedance), which are determined by local and regional structures of the electrical conductivity of the Earth's crust.

For the magnetic storm on November 12−14, 2012, a general regular trend of a decrease in intensity of the variations in both the geomagnetic field and GIC with increasing distance from the latitudes of the electrojet (the dominant external source of excitation of geoelectric fields in the region) is revealed (see Fig. 3). Visually, the $J(t)$ peaks for the GIC recorded at VKH station correlate quite well with dX/dt of the high-latitude IVA station (see Fig. 4). However, the characteristics of the corresponding $J(f)$ spectrum at high frequencies are much closer to the spectrum of $E_x(f)$ (the field synthesized for IVA based on the MT impedance of B50) than to the $X'(f)$ spectrum (see Fig. 5). This suggests a certain damping of the effects of intense high-frequency harmonics of geomagnetic variation due to the features of the local geoelectric section both in the synthesized E_x field and in actual GICs of VKH station (if we assume that the geomagnetic variations in IVA are an appropriate approximation of the geomagnetic field at VKH). Let us pay attention to the moderate value of the northern component of the MT response at B50 (in the range of 400−70 Ohm m, see Fig. 2b), and also, judging by the
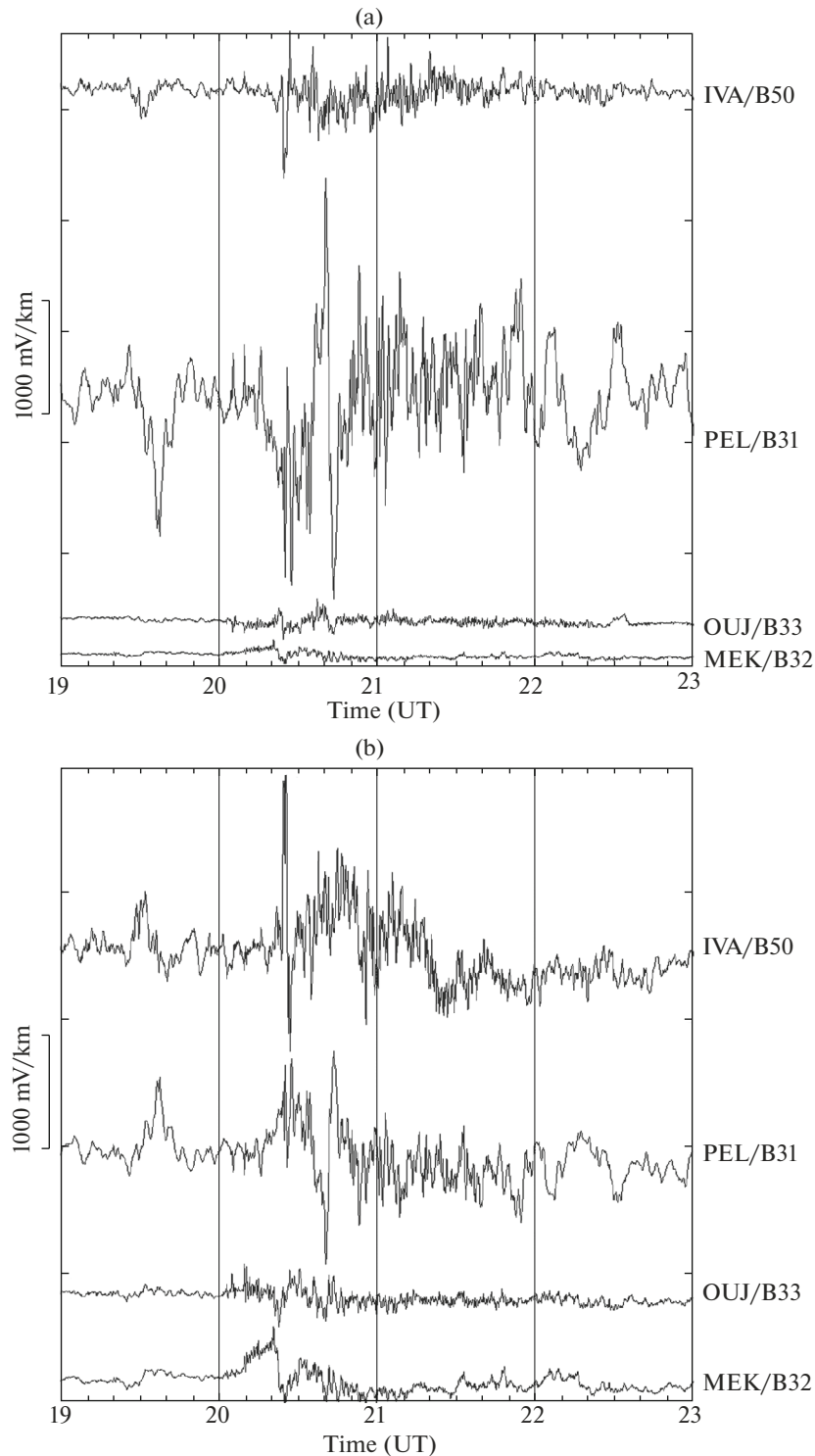
Fig. 11. Telluric fields (a) $E_x(t)$ and (b) $E_y(t)$, synthesized for the time interval of 19−23 UT on October 6, 2015, at IVA/B50, PEL/B31, OUJ/B33, and MEK/B32. The names of the stations after the slash indicate the MT sounding sites of the BEAR project, the impedances of which were involved in the synthesis.

distribution of S in Fig. 1, to a not too high crustal resistivity under VKH station.

When considering the storm of June 29, 2013, we used materials from PEL station, which coincides in position with B31 station of the BEAR project, whose MT impedance was involved in the synthesis of the local telluric field. Comparing the data presented in Figs. 6 and 7, it can be easily seen that, for close values

of geomagnetic variations at PEL and LOZ, the E_x variations at PEL increase significantly as compared to the E_x variations even at IVA and LOZ, located in higher latitudes. Apparently, the reason for this spatial pattern of the distribution of the telluric field is the local geoelectric heterogeneity at PEL, which facilitates a significant increase in the northern component of the MT impedance (see Figs. 2a, 2b). The spectral analysis of the data on this storm (see Fig. 9) demonstrates a smaller but also noticeable shift of the high-frequency part of the normalized spectrum $J(f)$ for RVD relative to the analogous $X'(f)$ spectrum at LOZ, closer to the $E_x(f)$ spectrum calculated from the impedance at B50. Note that, in this case, the data for all variations that were recorded almost at one site (at the closely located stations B50, LOZ, and RVD) were available for analysis (see Fig. 1).

Finally, for the third event, the substorm of October 6, 2015 (see Figs. 10−12), the influence of local geoelectric conditions on the character of variations in both the telluric field E_x and GIC at closely located stations is also revealed in the time and spectral domains: compare the electric fields of PEL and IVA with variations in the geomagnetic field that are close in intensity (see Fig. 10) and with the normalized $J(f)$ spectra for VKH, as well as the $dX(f)/dt(f)$ and $E_x(f)$ spectra for IVA.

Telluric Fields Induced by a Magnetic Storm of November 12−14, 2012, on the Ladoga Section of the Border of the Archean and Paleoproterozoic Geoblocks of the Shield

The results of a recent experiment of synchronous broadband magnetotelluric and magnetovariational soundings in the Northern Ladoga region (Sokolova et al., 2016) allow us to trace in good detail the spatial variations in the electric fields induced during intense space weather events along the profile line across the border of two shield geoblocks that differ greatly in geoelectric parameters: Archean Karelian craton and Proterozoic Svecofennian orogen (see Figs. 1, 14).

The regional contrast of typical values of the crustal conductivity of these blocks is enhanced by the presence in the bordering Raahe-Ladoga suture zone of a strong crustal conductor associated with the junction of the blocks along the northwest-southeastern Yanisyarvi deep fault (see Figs. 14, 15) (Kovtun, 1989; Zhamaletdinov et al., 2018). Estimates of the skin-layer thickness from the MT response values (see Figs. 2c, 15) at the points corresponding to the high-resistivity Archean "shoulder" of the contact (L03, L02) and the conductive suture zone of the Proterozoic part (L05, L07) for the period $T = 128$ s differ by almost an order of magnitude (60−100 and 4−10 km, respectively). Figure 14 shows the induction vectors for this period: invariants of magnetovariational transfer functions that connect the anomalous vertical magnetic field with the normal
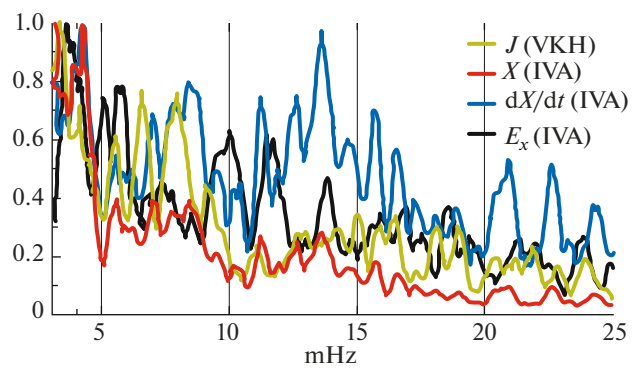

Fig. 12. Normalized spectra $X(f)$, $dX(f)/dt$, and $E_x(f)$ for IVA station and $J(f)$ for VKH station for the period of 19−23 UT on October 6, 2015.
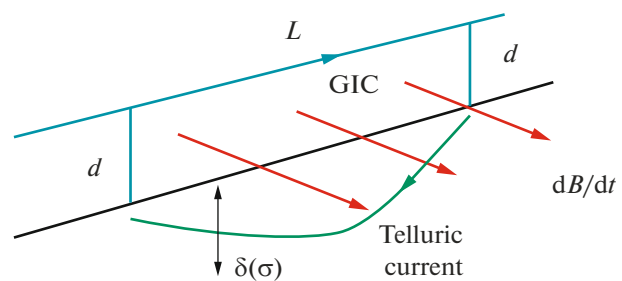
Fig. 13. Diagram of a GIC circuit of a grounded power transmission line: L is the length of the power line, d is the height of the supports, and $\delta(\sigma)$ is the depth of the effective telluric current (skin layer depth).

horizontal magnetic field (Berdichevsky and Dmitriev, 2009). Their spatial behavior indicates the presence in the suture zone at depths of 4−10 km of a region of increased electrical conductivity that concentrates anomalous telluric currents flowing in the northwest−southeast direction: the profile segment L07−L05−L03 is characterized by the minimum lengths of the induction vectors (they correspond to the minimum (zero) vertical magnetic field and the maximum horizontal one directly above the linear conductor). Further to the northeast along the profile, the vectors sharply increase on the insulating substrate and clearly line up in the northeast direction across the extension of the crustal conductor. This pattern closely agrees with the pseudosections of apparent resistivity (see Fig. 15); the results of 2D and 3D joint inversions of MT and MV data (Mints et al., 2018; Rokityansky et al., 2018) outline a thick southwest-inclined quasi-two-dimensional conducting zone with increased conductivity at depths of 5−15 km in this part of the Vyborg−Suoyarvi profile.

Figure 16 illustrates the results of the synthesis of the time series of telluric fields for the points of the L07−L02 profile segment during the geomagnetic storm of November 12−14, 2012, carried out using
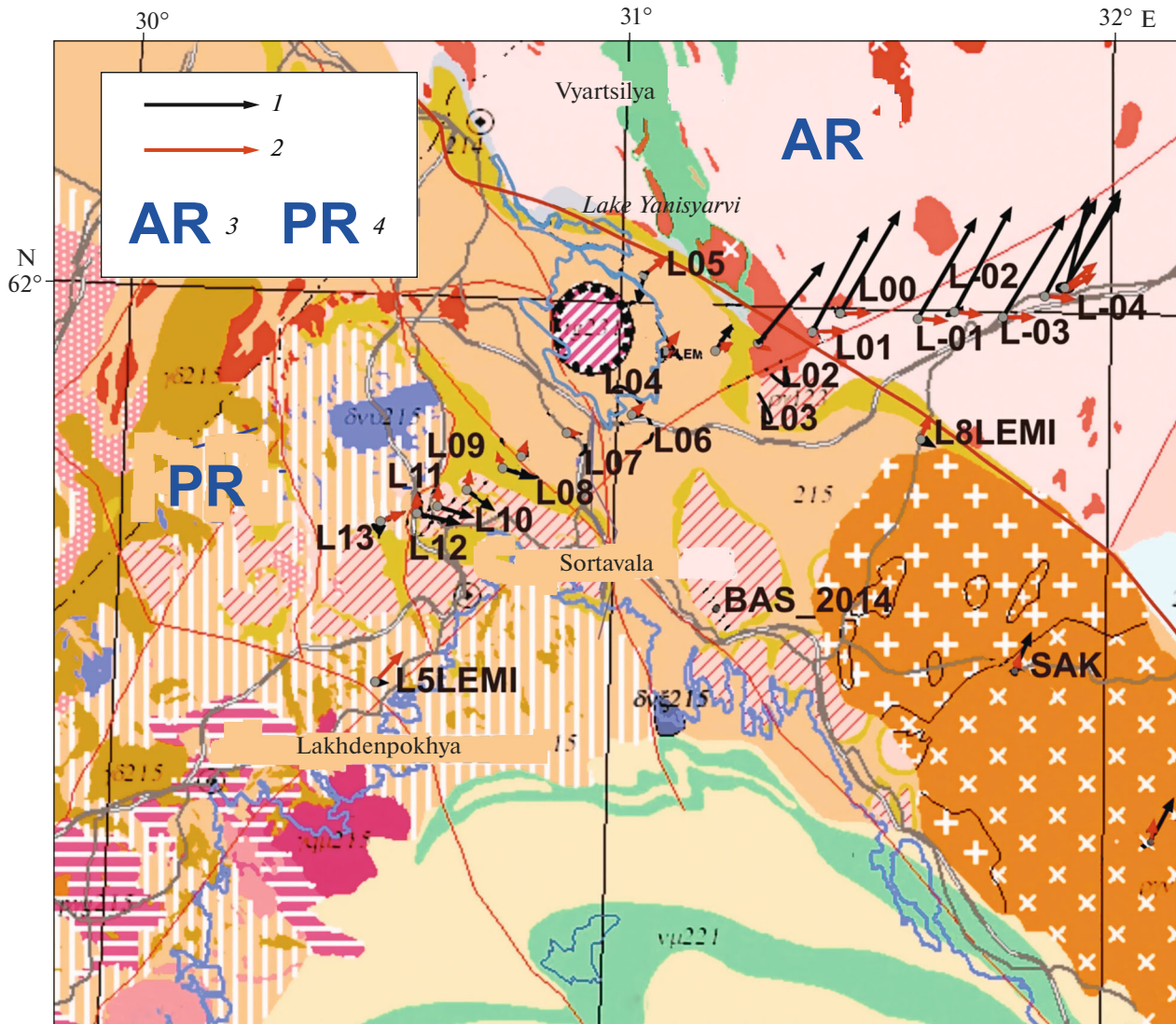
Fig. 14. Fragment of the geological map of Karelia for the territory of the Northern Ladoga (for a complete map and legend, see (Kulikov et al., 2017)) with superposition of magnetotelluric and magnetovariational sounding sites of the northeastern part of the Vyborg–Suoyarvi profile (Sokolova et al., 2016) and invariants of the magnetovariational response, i.e., induction vectors for a period of 125 s: (*1*) real; (*2*) imaginary. The vector scale is indicated by single arrows. (*3*) Archean geoblock; (*4*) Proterozoic geoblock.

local impedances and magnetic field records at MEK station of the IMAGE network. The Mekrijärvi observatory (MEK), which is considerably distant from the electrojet latitude, is characterized by a less-intensive variation in the magnetic field (see Fig. 3a) in the selected time interval of the ongoing storm; this is also true for the corresponding GIC record at the nearby KND station (Kandapoga) (see Fig. 3b). Telluric fields at all Ladoga sites under consideration correlate well with the MEK geomagnetic field and also with $J(t)$ at KND (see Figs. 16, 3a, and 3b, respectively). By the amplitudes of the variations, the stations are divided into two groups: sites with a Proterozoic substrate (they are characterized by minimal peak scatter: 0.2–0.3 V/km and less than 0.1 V/km at L05) and sites on the Archean base, comparable in the ampli-

tude range (0.5–1.2 V/km and up to 4 in E_y at L03) with the range of "synchronous" geoelectric fields at IVA/B50 (see Fig. 4). Close amplitudes of variations in both telluric components of this event according to the data of IVA/B50 and L03, most probably, are determined by the specific features of local impedance tensors (see Figs. 2a, 2c).

Thus, the analysis of the experimental material on the Northern Ladoga showed that the magnitude of the variations in the telluric field induced by the magnetic storm can vary by almost an order of magnitude at observation points located at fairly close distances, but within geological structures with significantly different geoelectric parameters.

Concluding the discussion, it is worth mentioning the evaluative character of the obtained estimates of the
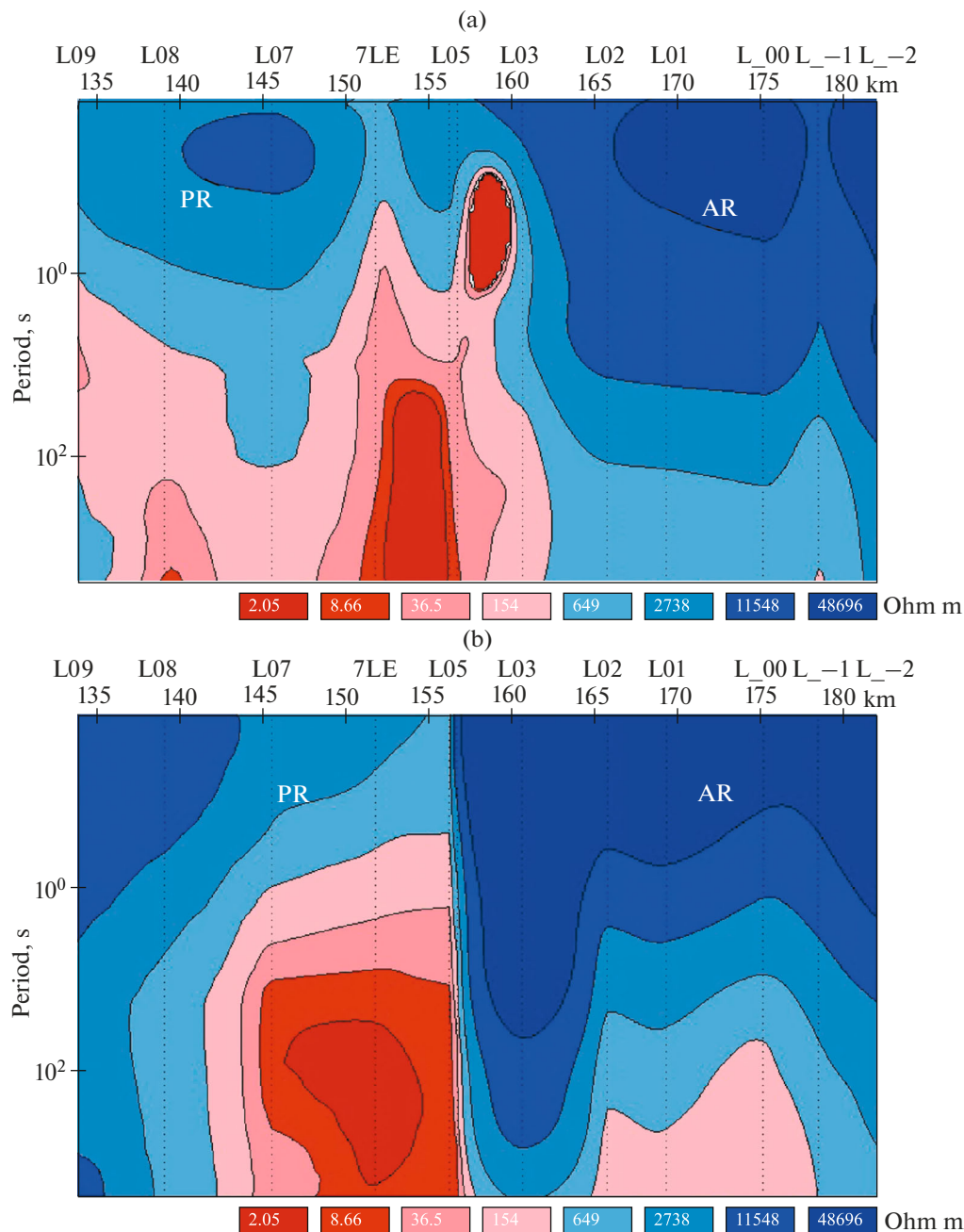
Fig. 15. Pseudosections (a) ρ_{xy} and (b) ρ_{yx} (in Ohm m according to the given color scale; x is the geographical north and y is the geographical east) along the northeastern segment of the Vyborg–Suoyarvi profile. For the profile position, see Figs. 1 and 14. AR is the Archean geoblock; PR is the Proterozoic geoblock.

electric fields induced in the Earth's crust of Fennoscandia by intense geomagnetic perturbations, i.e., effects of space weather anomalies. Let us address two determining factors: the limitations of the approach applied to the synthesis of the telluric field and the incompleteness of the data ensemble (in most cases, colocal geomagnetic and MT observations were absent).

(1) The plane-wave model of the induction excitation of the conductive Earth, which underlies the impedance relations of the geomagnetic and telluric

fields in the form (1), is valid for horizontal scales of an external source much greater than the corresponding skin depth. The model is certainly satisfied for large-scale ionospheric disturbances over well-conducting Earth surface (Berdichevsky and Dmitriev, 2009). However, under conditions of substantially inhomogeneous excitation sources, such as strongly localized current structures in the ionosphere (specifically, such rapid localized perturbations are often responsible for the GIC bursts (Yagova et al., 2018; Belakhovsky et al,
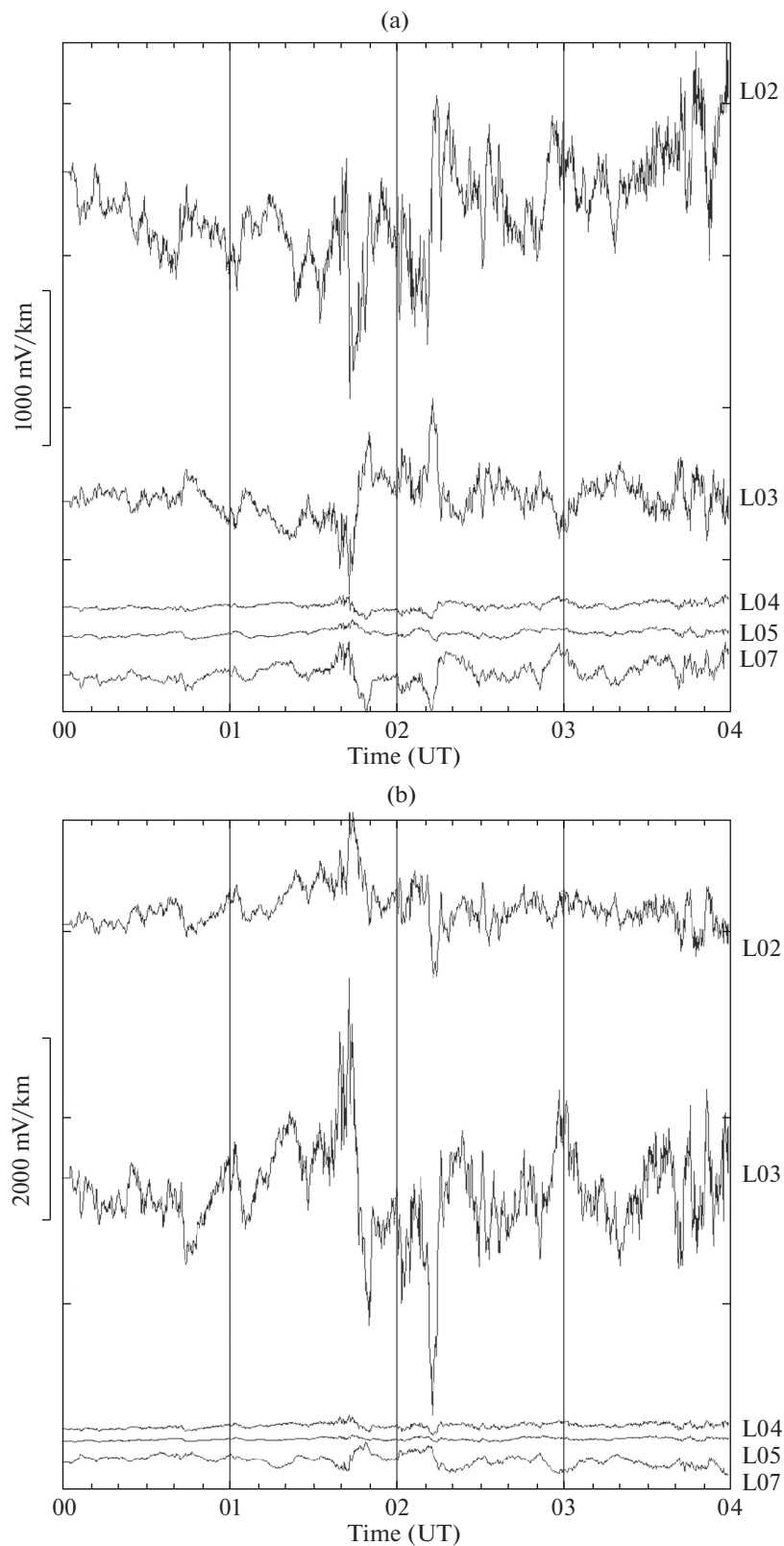
Fig. 16. Telluric fields (a) E_x and (b) E_y for five MT sounding sites of the segment of the Vyborg−Suoyarvi profile shown in Fig. 14. The fields are synthesized from the local estimates of MT responses at these sites using magnetic storm records of November 14, 2012, at the MEK station of the IMAGE network. The position of the profile and the MEK observatory is shown in Fig. 1; the positions of the sounding sites are shown in Fig. 14. The dependences of the estimates of the northern (xy) and eastern (yx) amplitude components of the impedance tensor on the period for these sites are shown in Fig. 2c.

2019)), above the highly resistive rocks of Fennoscandia, ratio (1) provides only the first approximation of the field relation. Therefore, estimating geoelectric fields with greater accuracy requires a numerical 3D modeling of the source structure, which is currently being developed for the regions of northern Europe (e.g., Ivannikova et al., 2018; Dimmock et al., 2019; and others).

(2) If, at a site with the MT impedance correctly estimated earlier, there are no permanent observations of telluric fields, but there are various intense geomagnetic events that satisfy the criterion of homogeneity of the external excitation (for example, in the case of a sufficient remote source), then the electric fields synthesized in model (1) based on the total tensor Z (in this case, the invariant of external excitation) will give fairly accurate local estimates of the induction responses suitable for further use to determine GICs, for example, when integrating the E field in the direction of the power line (taking into account its vector nature) over a network of sites of such estimates to determine the voltage between the ground, as in (Lukas et al., 2018). The actual anisotropy of the geoelectric structure will be embedded in the three-dimensional structure of the impedance tensor, which is characterized by comparable amplitudes of the main and additional Z components (like Z_{B31} in Fig. 2a). At the same time, the need to extrapolate geomagnetic observations over considerable distances in the absence of co-local MT and geomagnetic observations can introduce significant additional errors. The lateral heterogeneity of the electrical conductivity of the Earth's crust, distinct within the Fennoscandian shield (see Fig. 1), leads to the occurrence of abnormal geomagnetic responses (both in vertical and horizontal components) superimposed on the primary inducing fields.

The accounting for the totality of these factors would be guaranteed by full three-dimensional approach to constructing realistic magnetotelluric responses to space weather events. The essence of this approach is in modeling electromagnetic fields from the spatial distribution of anomalous structures of deep electrical conductivity excited by an inhomogeneous external source.

CONCLUSIONS

Based on the available regional magnetotelluric sounding data for a series of typical extreme space weather events (geomagnetic storms, substorms, and Pi3 pulsations recorded by the Scandinavian geomagnetic observation network IMAGE), the telluric (geoelectric) fields at a number of sites in high-latitude regions of the Russian northwest were estimated. The ability to make such estimations provides a background for predicting possible extreme values of GICs in grounded industrial infrastructure facilities, including regional power lines. In the approach used in our study, the calculations involved total local complex MT impedance tensors, which is a necessary condition for the reliable estimation of telluric fields at the observation sites, as well as the possibility of further analyzing their polarization and obtaining realistic estimates of the potential difference on the grounding points by integration (Lukas et al., 2018). However, the relationships between the input geomagnetic signal and the geoelectric response embedded in the algorithm for the synthesis of telluric fields were determined by the paradigm of a plane wave of an external source, while the magnetospheric and ionospheric events at high latitudes are characterized by heterogeneity of the latter (Engels et al., 2002; Sokolova et al., 2007). In addition, the extrapolation of the results of magnetotelluric and geomagnetic observations requires additional verification in the presence of sharp inhomogeneities in the structure of electrical conductivity. For example, Rokityansky et al. (2018) already analyzed estimates of the actual values of anomalous magnetic fields over the conductive suture zone in Northern Ladoga. Appropriate corrections can and should be taken into account when using the geomagnetic observations at the MEK station as the base for obtaining estimates of telluric fields in South Karelia and the Ladoga region and modeling GICs in the nearby Kandapoga (KND) based on these estimates. The implementation of the latter statement, as well as 3D modeling of telluric responses based on the available data on the volume distribution of the region's electrical conductivity using adequate external source models, is the immediate prospect of our further research.

At the same time, already at the present stage of the study, the calculated telluric fields have shown a good correlation with the observed GICs in the power transmission lines of Karelia and the Kola Peninsula. A joint analysis of all three types of variations made it possible to draw important conclusions regarding the variability of geomagnetic and telluric fields in the region of central and eastern Fennoscandia related to the GIC hazard. It was shown that the regional features of the deep electrical conductivity of various geological provinces, as well as its local inhomogeneities, make a significant contribution to the spatial variations of electromagnetic responses to space-weather disturbances and overlap with the regular trend of decreasing amplitudes when moving away from auroral latitudes. Based on the experimental data, it was traced how, when passing from the moderately conductive geoblock of the Svecofennian orogen to the region of the highly resistive Archean crust of the Karelian craton, the telluric field variations sharply increase, at some sites reaching the values typical of high-latitude stations. At the same time, the zones with increased integral crustal conductivity (small skin depth) are distinguished by markedly weakened variations. Magnetotelluric impedance plays the role of a low-pass filter, which, with its relative smallness (high underground conductivity), suppresses the high-frequency components in the spectra of geoelectric fields in comparison

with the spectrum of the inducing magnetic field variations (geomagnetic field variability *dB/dt*).

We hope that our research will draw the attention of specialists involved in the problem of the assessment of GIC effects arising in technological systems during space weather anomalies to the need for additional magnetotelluric observations in regions that are influenced by these effects and have significant heterogeneity of the geoelectric structure.

CONFLICT OF INTEREST

The authors declare to have no conflict of interest.

REFERENCES

Alekseev, D., Kuvshinov, A., and Palshin, N., Compilation of 3D global conductivity model of the Earth for space weather applications, *Earth, Planets Space,* 2015, vol. 67 (108).
https://doi.org/10.1186/s40623-015-0272-5

Allen, J., Frank, L., Sauer, H., and Reiff, P., Effects of the March 1989 solar activity, *Eos, Trans. Amer. Geophys. Union*, 1989, vol. 70 (46), pp. 1486−1488.

Belakhovsky, V.B., Pilipenko, V.A., Sakharov, Ya.A., and Selivanov, V.N., Characteristics of the variability of a geomagnetic field for studying the impact of the magnetic storms and substorms on electrical energy systems, *Izv., Phys. Solid Earth,* 2018, vol. 54, no. 1, pp. 52−65.

Berdichevsky, M.N. and Dmitriev, V.I., *Modeli i metody magnitotelluriki* (Models and Methods of Magnetotellurics) (Moscow: Nauchnyi Mir, 2009).

Cannon, P., Angling, M., Barclay, L., Curry, C., Dyer, C., Edwards, R., Greene, G., Hapgood, M. A., Horne, R. B., Jackson, D., Mitchell, C., Owen, J., Richards, A., Ryden, K., Saunders, S., Sweeting, M., Tanner, R., Thomson, A., and Underwood, C., in *Extreme Space Weather: Impacts on Engineered Systems and Infrastructure* (London: Royal Academy of Engineering, 2013), pp. 1−68.

Dimmock, P., Rosenqvist, L., Hall, J.O., Viljanen, A., Yordanova, E., Honkonen, I., André, M., and Sjöberg, E.C., The GIC and geomagnetic response over Fennoscandia to the 7−8 September 2017 geomagnetic storm, *Space Weather,* 2019, vol. 17, no. 7, pp. 989−101.

Engels, M., Korja, T., and BEAR working group, Multisheet modelling of the electrical conductivity structure in the Fennoscandian Shield, *Earth, Planets Space,* 2002, vol. 54, pp. 559−573.
https://doi.org/10.1186/BF03353045

Epishkin, D.V., Improving magnetotelluric data-processing methods, *Vestn. Mosk. Univ., Ser. 4: Geol.*, 2016. vol. 71, no. 5, pp. 347−354.

Ernst, T., Sokolova, E.Yu., Varentsov, Iv.M., and Golubev, N.G., Comparison of two MT-data processing techniques using synthetic data sets, *Acta Geophys. Pol.,* 2001, vol. 49, no. 2, pp. 213−243.

Eroshenko, E.A., Belov, A.V., Boteler, D., Gaidash, S.P., Lobkov, S.L., Pirjola, R., and Trichtchenko, L., Effects of strong geomagnetic storms on Northern railways in Russia, *Adv. Space Res.,* 2010, no 46, pp. 1102−1110.

Forbes, K.F. and Cyr, O.C.St., Solar activity and economic fundamentals: evidence from 12 geographically disparate power grids, *Space Weather,* 2008, vol. 6. s10003.
https://doi.org/10.1029/2007SW000350

Glubinnoe stroenie i seismichnost' Karelo-Kol'skogo regiona i ego obramleniya (Deep Structure and Seismicity of the Karelia−Kola Region and Its Surroundings) Sharov, N.V, Ed., (Petrozavodsk: KarNTs RAN, 2004).

Ivannikova, E., Kruglyakov, M., Kuvshinov, A., Rastätter, L., and Pulkkinen, A., Regional 3D-modeling of ground electromagnetic field due to realistic geomagnetic disturbances, *Space Weather,* 2018, vol. 16, no. 5, pp. 476−500.
https://doi.org/10.1002/2017SW001793

Kelbert, A., Balch, C.C., Pulkkinen, A., Egbert, G.D., Love, J.J., Rigler, E.J., and Fujii, I., Methodology for time-domain estimation of storm time geoelectric field using the 3-D magnetotelluric response tensors, *Space Weather,* 2017, vol. 15, no. 7, pp. 874−894.
https://doi.org/10.1002/2017SW001594

Kelly, G.S., Viljanen A., Beggan, C., Thomson, A.W.P., and Ruffenach, A., Understanding GIC in the UK and French high voltage transmission systems during severe magnetic storms, *Space Weather,* 2017, vol. 15, no. 1, pp. 99−114.

Kleimenova, N.G. and Kozyreva, O.V., Magnetic storms and heart attacks: are the storms always dangerous?, *Geofiz. Prots. Biosfera,* 2008, vol. 7, no. 3, pp. 5−24.

Knipp, D.J., Synthesis of geomagnetically induced currents: Commentary and research, *Space Weather,* 2015, vol. 13, pp. 727−729.

Korja T., Engels, M., Zhamaletdinov, A.A., Kovtun, A.A., Palshin, N.A., Smirnov, M.Yu., Tokarev, A.D., Asming, V.E., Vanyan, L.L., Vardaniants, I.L. and the BEAR Working Group, Crustal conductivity in Fennoscandia—a compilation of a database on crustal conductance in the Fennoscandian Shield, *Earth, Planets*

Space, 2002, vol. 54, pp. 535–558.
https://doi.org/10.1186/BF03353044

Kovtun, A.A., *Stroenie kory i verkhnei mantii na severo-za-pade Vostochno-Evropeiskoi platformy po dannym mag-nitotelluricheskikh zondirovanii* (Crust and Upper Mantle Structure in the Northwest of the Eastern European Platform according to Magnetotelluric Sounding Data), Leningrad: Izd-vo LGU, 1989.

Kozyreva, O.V., Pilipenko, V.A., Belakhovsky, V.B., and Sakharov, Ya.A., Ground geomagnetic field and GIC response to March 17, 2015 storm, *Earth, Planets Space,* 2018, vol. 70(157).
https://doi.org/10.1186/s40623-018-0933-2

Kulikov, V.S., Svetov, S.A., Slabunov, A.I., Kulikova, V.V., Polin, A.K., Golubev, A.I., Gor'kovets, V.Ya., Ivash-chenko, V.I., and Gogolev, M.A., The 1: 750000 Geo-logical Map of the southeastern Fennoscandia: new ap-proaches to compilation, in *Tr. Karel. NTs RAN. Ser. Geol. Dokembriya* (Proc. Karelian Res. Center Rus. Acad. Sci. Ser. Precambrian Geol.), 2017, no. 2, pp. 3–41.
https://doi.org/10.17076/geo444

Lanzerotti, L.J., Space weather effects on technologies, in *Space Weather, AGU Geophys. Monogr. Ser.,* vol. 125, Song, P., Singer, H.J., and Siscoe, G.L., Eds., Wash-ington: AGU, 2001, pp. 11–22.

Love, J.J., Pulkkinen, A., Bedrosian, P.A., Jonas, S., Kel-bert, A., Rigler, E.J., Finn, C.A., Balch, C.C., Rut-ledge, R., Waggel, R.M., Sabata, A.T., Kozyra, J.U., and Black, C.E., Geoelectric hazard maps for the con-tinental United States, *Geophys. Res. Lett.,* 2016, vol. 4, pp. 9415–9420.
https://doi.org/10.1002/2016GL070469

Lucas, G.M., Love, J.J., and Kelbert, A., Calculation of voltages in electric power transmission lines during his-toric geomagnetic storms: An investigation using realis-tic earth impedances, *Space Weather,* 2018, vol. 16, pp. 185–195.
https://doi.org/10.1002/2017SW001779

Mints, M.V., Sokolova, E. Yu, and the LADOGA working group, 3D model of the deep structure of the Svecofen-nian Accretionary Orogen based on data from CDP seismic reflection method, MT sounding and density modeling, in *Tr. Karel. NTs RAN. Ser. Geol. Dokembriya* (Proc. Karelian Res. Center Rus. Acad. Sci. Ser. Pre-cambrian Geol.), 2018, no. 2, pp. 34–61.
https://doi.org/10.17076/geo656

Pellinen, R.J., and Heikkila, W.J., Inductive electric fields in the magnetotail and their relation to auroral and substorm phenomena, *Space Sci. Rev.,* 1984, vol. 37, pp. 1–61.

Pirjola, R., Kauristie, K., Lappalainen, H., Viljanen, A., and Pulkkinen, A., Space weather risk, *Space Weather,* 2005, vol. 3, p. S02A02.

Pulkkinen, A., Pirjola, R., Boteler, D., Viljanen, A., and Yegorov, I., Modeling of space weather effects on pipe-lines, *J. Appl. Geophys.,* 2001, vol. 48, p. 233–256.
https://doi.org/10.1016/S0926-9851(01)00109-4

Pulkkinen, A.A., Bernabeu, E., Thomson, A., Viljanen, A., Pirjola, R., Boteler, D., Eichner, J., Cilliers, P.J.,

Welling, D., Savani, N.P., Weigel, R.S., Love, J.J., Balch, Ch., Ngwira, C.M., Crowley, G., Schultz, A., Kataoka, R., Anderson, B., Fugate, D., Simpson, J.J., and MacAlester, M., Geomagnetically induced cur-rents: Science, engineering and applications readiness, *Space Weather,* 2015, no. 15, pp. 828–856.

Pulkkinen, A., Lindahl, S., Viljanen, A., and Pirjola, R., Geomagnetic storm of 29–31 October 2003: Geomag-netically induced currents and their relation to prob-lems in the Swedish high-voltage power transmission system, *Space Weather,* 2005, no. 3, p. S08C03.
https://doi.org/10.1029/2004SW000123

Pulkkinen, A.A., Bernabeu, E., Thomson, A., Viljanen, A., Pirjola, R., Boteler, D., Eichner, J., Cilliers, P.J., Well-ing, D., Savani, N.P., Weigel, R.S., Love, J., Balch, Ch., Ngwira, C.M., Crowley, G., Schultz, A., Kataoka, R., Anderson, B., Fugate, D., Simpson, J.J., and MacAl-ester, M., Geomagnetically induced currents: Science, engineering and applications readiness, *Space Weather,* 2017, no. 15, pp. 828–850.

Püthe, C. and Kuvshinov, A., Towards quantitative assess-ment of the hazard from space weather: Global 3D-modellings of the electric field induced by a real-istic geomagnetic storm, *Earth, Planets Space,* 2013, vol. 65, pp. 1017–1025.

Rokityansky, I.I., Sokolova, E.Yu., Tereshin, A.V., Yakov-lev, A.G., and the LADOGA working group, Electrical conductivity anomalies in the contact zones of Archean and Proterozoic geoblocks on the Ukrainian and Baltic Shields, *Geofiz. Zh.,* 2018, vol. 40, no. 5, pp. 209–244.
https://doi.org/10.24028/gzh.0203-3100.v40i5.2018.147490

Sakharov, Ya.A., Danilin, A.N., and Ostafiychuk, R.M., Registration of GIC in power systems of the Kola Pen-insula, *Proc of 7th International symposium on Electro-magnetic Compatibility and Electromagnetic Ecology, St-Petersburg, June 26–29, 2007,* St-Petersburg, 2007, pp. 291–293.

Sakharov, Ya.A., Kudryashova, N.V., Danilin, A.N., Kokin, S.M., Shabalin, A.N., and Pirjola, R., The ef-fect of geomagnetic perturbation on the performance of railroad automatics, *Vestnik MIIT,* 2009, no. 21, pp. 107–111.

Sokolova, E.Yu., Golubtsova, N.S., Kovtun, A.A., Ku-likov, V.A., Lozovsky, I.N., Pushkarev, P.Yu., Roki-tyansky, I.I., Taran, Ya.V., and Yakovlev, A.G., Re-sults of synchronous magnetotelluric and magnetovaria-tional soundings in the area of the Ladoga conductivity anomaly, Geofizika, 2016, no. 1, pp. 48–64.

Sokolova, E.Yu., Varentsov, I.M., and BEAR working group, Deep array electromagnetic sounding on the Baltic Shield: External excitation model and implica-tions for upper mantle conductivity studies, *Tectono-physics,* 2007, vol. 445, pp. 3–25.

Torta, J.M., Marsal, S., and Quintana, M., Assessing the hazard from geomagnetically induced currents to the entire high-voltage power network in Spain, *Earth, Planets Space*, 2014, vol. 66, no. 87.
https://doi.org/10.1186/1880-5981-66-87

Torta, J.M., Marcuello, A., Campanyà, J., Marsal, S., Queralt, P., and Ledo, J., Improving the modeling of geomagnetically induced currents in Spain, *Space Weather,* 2017, no. 15.
https://doi.org/10.1002/ 2017SW001628

Vakhnina, V.V., Kuvshinov, A.A., Shapovalov, V.A., Chernenko, A.N., and Kretov, D.A., The development of models for assessment of the geomagnetically induced currents impact on electric power grids during geomagnetic storms, *Adv. Electr. Comput. Eng.,* 2015, no. 15, pp. 49−54.

Varentsov, Iv.M. Sokolova, E.Yu., Martanus, E.R., Nalivaiko, K.V., and the Working Group of the BEAR project, Methodology of the construction of transfer operators of the electromagnetic field for the array of synchronous BEAR soundings, *Fiz. Zemli,* 2003, no. 2, pp. 30−61.

Viljanen, A., The relation between geomagnetic variations and their time derivatives and implications for estimation of induction risks, *Geophys. Rev. Lett.,* 1997, vol. 24, pp. 631−634.

Viljanen, A., Nevanlinna, H., Pajunpaa, K., and Pulkkinen, A., Time derivative of the geomagnetic field as an activity indicator, *Ann. Geophys.,* 2001, vol. 19, pp. 1107−1118.

Yagova, N.V., Pilipenko, V.A., Fedorov, E.N., Lhamdondog, A.D., and Gusev, Yu.P., Geomagnetically induced currents and space weather: Pi3 pulsations and extreme values of time derivatives of the geomagnetic field's horizontal components, *Izv., Phys. Solid Earth,* 2018, vol. 54, no. 5, pp. 749−763.

Yermolaev, Yu.I., Yermolaev, M.Yu., Zastenker, G.N., Zelenyi, L.M., Petrukovich, A.A., and Sauvaud, J.-A., Statistical studies of geomagnetic storm dependencies on solar and interplanetary events: A review, *Planet, Space Sci.,* 2005, vol. 53, pp. 189−196.

Zhamaletdinov, A.A., Kolesnikov, V.E., Skorokhodov, A.A., Shevtsov, A.N., Nilov, M.Yu., Ryazantsev, P.A., Sharov, N.V., Birulya, M.A., and Kiryakov, I.A., Results of electric profiling using direct current in combination with AMT sounding along the profile across the Lake Ladoga Anomaly, *Tr. Kar NTs RAN,* 2018, no. 2, pp. 91−110.

Translated by M. Chubarova